




## Research Article

# Evaluation of machining performance and multi criteria optimization of novel metal-Nimonic 80A using EDM

Vikas K. Shukla<sup>1</sup> · Rakesh Kumar<sup>1</sup> · Bipin Kumar Singh<sup>2</sup> 

Received: 13 August 2020 / Accepted: 24 December 2020 / Published online: 12 February 2021

© The Author(s) 2021 

## Abstract

This study focused to machine novel Nimonic 80A through Electric Discharge Machine process. The process parameters are optimised to achieve high surface integrity along with high material removal rate (MRR) with minimum energy consumption. Central composite design along with analysis of variance technique has been applied to make correlation between the process parameter and responses. The developed model of surface roughness shows that the peak current and pulse-on time have significant effect whereas; a little effect of pulse-off time. The said result may be obtained due to simultaneous action of deposition and notching (removal) of material in order to form crater. In case of MRR, the pulse-on time and peak current are found as significant factors with increasing trend (i.e. when the input values are increased the MRR increases) whereas; a reverse trend is noticed with pulse-off time. The optimum values for maximum MRR (0.512444 gm/min) and minimum surface roughness (7.82203  $\mu\text{m}$ ) with 81% desirability are obtained for the process parameter as 13.49 A peak current, 150  $\mu\text{s}$  pulse-on time and 4  $\mu\text{s}$  pulse-off time.

**Keywords** Electric discharge machining (EDM) · NIMONIC 80A · Material removal rate (MRR) · Surface roughness (SR) · Response surface methodology (RSM)

## 1 Introduction

The inventions of super alloys to accomplish the demand of modern industries create various problems for the manufacturing industries. These super alloys are rarely machined with conventional machining process. Nimonic 80A is one of the super alloy which consumes a lot of energy and very difficult to machine. Hence, to machine these kinds of materials, new processes showing better performance have been invented by the researchers. These materials have many application in advance industries like aeronautic, automobile, nuclear reactor, missile, turbine, chemical etc. for fabrication of various components. Some major applications of Nimonic 80A are in the nuclear generators, bolts, tube, gas-turbine components discs, exhaust

valves, off shore/marine automotive, engines and electrical applications. Therefore, it is very indeed to investigate a low expense machining process for these materials that provides better surface integrity and consume low energy. Hence, an attempt has been made with electric discharge machining (EDM) to optimise the machining parameters in order to earn maximum profits. In EDM process electrode plays a vital role on the machining performance, so its selection is an important task. Guha et al. [1] carried out various experiments with different electrode used in EDM to machine copper beryllium alloys. The results illustrated that the positive polarity copper electrode had maximum material removal rate (MRR) whereas, for negative polarity, the highest MRR was obtained with graphite electrode. Another analysis for fatigue experiment on EDM

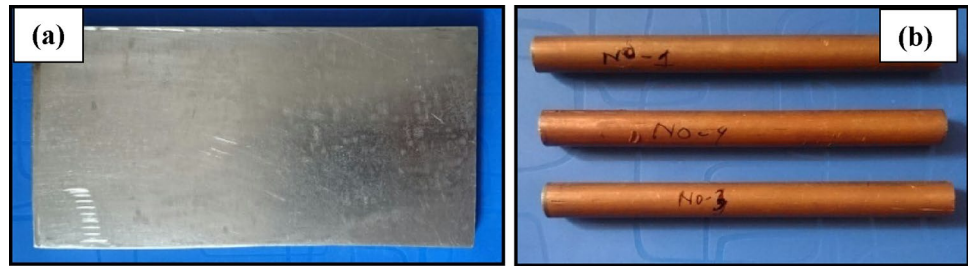
✉ Bipin Kumar Singh, bipin.k.singh@goel.edu.in; bipinmech2008@gmail.com | <sup>1</sup>Department of Mechanical Engineering, Sant Longowal Institute of Engineering And Technology, Sangrur, Punjab 148106, India. <sup>2</sup>Department of Mechanical Engineering, Goel Institute of Technology and Management, Lucknow, Uttar Pradesh 713209, India.



for AISID6 tool steel with varying machining parameters was carried out by Abu Zeid et al. [2]. The results clearly showed that the pulse-on time had almost negligible effect while peak current have remarkable effect on the surface roughness. Singh et al. [3] selected composite of AL-MMC having 10% SiCp to carry out various machining experiments on EDM. Pulse current, flushing pressure and pulse-on time were considered as input parameters whereas, MRR, tool wear rate (TWR), radial overcut and surface roughness were output parameters. The results showed that the MRR was increased with increase in current and pulse-on time due to higher thermal loading on both electrodes. Longer pulse duration also resulted in the larger removal per discharge, but due to formation of larger crater higher surface roughness was noticed. Liao and Yu [4] selected carbon-carbon composite to determine the optimal setting for process parameters on the EDM. The MRR was increased by setting parameters at their highest values. The pulse-on time, peak current and gap voltage have significant effect on the behaviour of electrode wear rate and MRR. Numerical model for temperature distribution to predict its behaviour during electrical discharge process was investigated by Salah et al. [5]. Results of experiments concluded that the conductivity had significant effect on temperature distribution. Therefore, the conductivity was considered as a crucial factor for accuracy. Kanlayasiri et al. [6] used wire-EDM process to investigate the effects of input variables on the surface integrity during machining of DC53 die steel. The analysis of results showed that peak current and pulse-on time were the significant input parameters that affect the surface integrity. Multiple regression methods were used to formulate the mathematical model of pulse-on time and peak current for prediction of surface integrity. Joshi et al. [7] observed optimal ranges of the input parameters during roughing and finishing operation. The observation clearly revealed that the modelling and optimization was an effective tool for process engineer to select the optimum conditions for high productivity and good surface finish during EDM process. Singh et al. [8] investigated the surface integrity of H11 steel on EDM using copper tool electrode. It was observed that negative polarity of tool electrode was a desirable factor to improve the value of surface integrity. The investigation also showed that the suspension of particles in a dielectric fluid improved the quality of surface whereas, higher peak currents produces rougher surface during EDM process. Govindan et al. [9] used dry electrical discharge machining to study the analysis of micro cracks generated on the machined surface. It was observed that pulse-off time, voltage, current shield clearance and speed were the controlling factors at the wall region that controls the formation of average density of micro-crack. Whereas, pressure (P) and current (I) were

the controlling parameters in the bottom region to control the average crack density. The analysis of results revealed that the mechanism of micro-crack formation was better represented in terms of average crack length rather than the crack number density. Singh and Yeh [10] used gray relational co-efficient technique to optimize the APM-EDM process for minimum tool wear rate, maximum MRR and better surface integrity. Pulse-on time was considered as the significant factor among the other input process parameters. The optimal parameter setting of the eight factors A1B1C3D2E3G3H2 was found to achieve maximum responses. Shayan et al. [11] developed empirical models using analysis of variances (ANOVA) to establish relationships between process factors and responses. It was concluded that the pulse-on time was the significant factor having profound effect on the cutting rate and surface integrity for cemented tungsten carbide electrode. Sahu et al. [12] used ADEA approach to optimize the various responses during EDM of AISI D2 steel. The analysis of results showed best surface quality as well as productivity with  $I_p = 7$  amp,  $T_{on} = 200$   $\mu$ s,  $t = 90\%$ , and  $F_p = 0.4$  kg/cm. The result also showed maximum MRR as  $13.900$  mm<sup>3</sup>/min, TWR as  $0.0201$  mm<sup>3</sup>/min and surface roughness  $R_a$  as  $4.9300$   $\mu$ m. Goswami et al. [13] used WEDM process for machining of Nimonic 80A to investigate the surface integrity, MRR and wire wear ratio. The effect on microstructure of the samples after machining was analysed through scanned electron microscopy (SEM). The analysis found pulse-off time ( $T_{off}$ ) and pulse-on time ( $T_{on}$ ) were noteworthy factors for prediction of MRR. The analysis also showed that the wire deposition on the machined surface was found too below at lower values of pulse-on time and higher value of pulse-off time. A review on the influence of process parameter for EDM process was published by Muthuramalingam et al. [14]. The study discussed an overview of the EDM process and the performance in terms of MRR, surface roughness and electrode wear rate. The analysis used pulse shape, discharge energy and electrical variable as input variables. Recently, Sahu et al. [15] used EDM process for machining of Nimonic 80A. Researchers selected only two factor i.e. peak discharge current and pulse-on duration to see their effect on material removal efficiency, minimal tool wear rate, and surface integrity. The researchers found optimum values for surface roughness as  $14.1$   $\mu$ m, MRR as  $9.05 \times 10^{-3}$  g/s, tool wear rate as  $1.2 \times 10^{-5}$  g/s when peak discharge current was 35 A and pulse-on duration was 1000  $\mu$ s. Furthermore, a number of researches were carried out by Huu et al. [16–18] that illustrates different optimisation processes during EDM machining.

Therefore, the above literatures clearly suggests that a little emphasis has been made to analyze the machining performance of super-alloy like Nimonic 80A using EDM

**Fig. 1** **a** Work material Nimonic 80A plate **b** copper electrode**Table 1** Composition of work material

Ni %	C%	Cr%	Fe%	Zr%	Co%	Mn%	Si%	Br%	S%	Ti%
73.29	0.013	19.58	2.19	0.15	0.2	0.77	1.0	0.02	0.015	2.58

**Table 2** Properties of Nimonic 80A

Properties of Nimonic 80A	Values
Tensile strength	1000 MPa
Compressive strength	2200 Mpa
Hardness	250–300 HV
Maximum temperature resistance for oxidation and scaling	815 °C
Properties of electrode (Copper)	
Density	8.9 kg/m <sup>3</sup>
Electrical resistivity	0.0167 Ωmm <sup>2</sup> /m
Melting point	1083 °C

process under the criteria of minimum energy consumption. Hence, in this investigation, at first, the experimental design are planned according to three factor three level central composite design (CCD) using design expert software. Then after, the models of MRR and surface roughness are developed through ANOVA analysis. The developed model are thoroughly investigate to make co-relationship between the machining parameter like peak current, pulse-on time and pulse-off time on the responses like surface integrity and high MRR. At last, an optimum set of input parameter has been postulated that consume the minimum energy to give maximum MRR along with minimum surface roughness.

## 2 Experimental details

In this investigation, Nimonic 80A (Supplier: South Asia Metal & Alloy) having dimension 140X80X8 mm was selected as workpiece to carried out the machining operations. The picture of same is shown in Fig. 1a. The compositions as well as properties of Nimonic 80A are listed in Tables 1 and 2. Electrolytic copper (99.99% purity) having diameter 10 mm and length 25 mm was selected as

**Fig. 2** SPARKONIXS50ZNC EDM Machine

electrode material as shown in Fig. 1b. The properties of electrode are also shown in Table 2. SPARKONIXS50ZNC EDM machine was used to carry out the machining experiments. A pictorial view of the EDM machine is shown in Fig. 2. The detailed specifications of EDM are listed in Table 3.

This investigation comprised, three level of process parameter i.e. peak current ( $I_p$ ), pulse-off time ( $T_{off}$ ) and pulse-on time ( $T_{on}$ ) to conduct the experiments. The three levels of process parameters are shown in Table 4. RSM technique was selected to carry out the experimental investigation using design expert software. In this technique, a number of quantitative data were selected from appropriate experiments to solve the multi variable equations through correlating the dependent parameters i.e. responses like MRR and surface roughness with independent parameters i.e. input variables like  $I_p$ ,  $T_{on}$  and  $T_{off}$ . The number of treatment were based on face centered composite second order design having variable ( $K=3$ ), Factorial point ( $2^k=8$ ), star points ( $2^k=6$ ), Center points ( $n=5$ ) and  $\alpha$  (1.0). This gives a total of 19 degree of freedom for three process parameters. The evaluation of MRR after machining is also very important for productivity, so

**Table 3** Specifications of SPARKONIXS50ZNCEDM machine

Specifications of EDM Machine	
Machining unit	S50(ZNC)
Tank size (mm)	900 × 550 × 357
Table size (mm)	600 X 400
Long-cross travel (mm)	350 × 2 × 25
Vertical filter	14",10 MICRON
Quill (mm)	250
Max. height of work piece (mm)	350
Max. weight of work piece (Kg)	550
Dielectric fluid	CPC KEROSENE
Max. electrode weight (Kg)	35
Parallelism of table surface with travel	0.02
Sequences of the electrode travel	0.02/300
Motor for pump(HP)	1
Power connects (KVA)	415 V, 3 Phase, 50 Hz

special care was taken during weighing process. The MRR is calculated by weighing the work-piece material before and after machining. The weight difference was divided by machining time to evaluate MRR which is shown in Eq. 1. Another response parameter i.e. surface roughness after machining was measured according to ISO 4287 on SURTRONIC 25 (Make: Taylor Hobson, Japan). After, every pass of machining the surface roughness was measured. The direction to measure the surface roughness is parallel to the cutting velocity vector. An average of ten reading is taken to cite the value of surface roughness in order to minimize the error. A cut-off length 0.8 mm (0.03 in) is used to measure the surface roughness.

$$MRR = \frac{W_1 - W_2}{T} \tag{1}$$

where  $W_1$  = Wt. of material before machining (in grams).  
 $W_2$  = Wt. of material removal after machining (in grams).  
 $T$  = Duration of machining (min.)

In this work, multiple regression equations in terms of mathematical models were developed using RSM for the quality characteristics of machined parts. A detailed description of RSM was illustrated earlier by Singh et al. [19–22]. The second order response after machining for the different input variables has been assumed as:

$$Y = \beta_0 \sum_{i=1}^k \beta_{ix_i} + \sum_{i=1}^k \beta_{iix_i^2} + \sum_{i<j} \beta_{ijx_ix_j} + \varepsilon \tag{2}$$

$i = 1, \dots, k$   
 $j = 2, \dots, k$ .where

$Y$  = Response variable ex. surface roughness and MRR.  
 $X_i, X_j$  = independent factors such as peak current, pulse-off time and pulse-on time.

$K$  = number of factors.  
 $\varepsilon$  = Error.

For three factors the above equation can be explained as:

$$Y = \beta_0 + \beta_1 X_1 + \beta_2 X_2 + \beta_3 X_3 + \beta_{11} X_1^2 + \beta_{22} X_2^2 + \dots + \beta_{12} X_1 X_2 + \beta_{13} X_1 X_3 + \dots + \varepsilon \tag{3}$$

Model can be expressed in matrix notation as:-

$$Y = bX + \varepsilon \tag{4}$$

$Y$  = Response,  $\varepsilon$  = Error.  
 In the matrix notation

$$b = (X' \cdot X)^{-1} \cdot (X' \cdot Y)$$

The above Eq. (2), (3) and (4) was used to determine the coefficients. All the regression coefficients of the models were computed as above for different parameters, viz., peak current, pulse-off time and pulse-on time. The levels of process parameters are demonstrated in Table 4.

### 3 Results and discussion

The experimental values of MRR and surface roughness at different set of process parameters after machining of Nimonic 80A are shown in Table 5. Figure 3 represents the images of all machined surfaces developed after machining. To develop different models of MRR and surface roughness the values of MRR and surface roughness were selected from Table 5.

#### 3.1 Effect of peak current, pulse-on time and pulse-off time on MRR

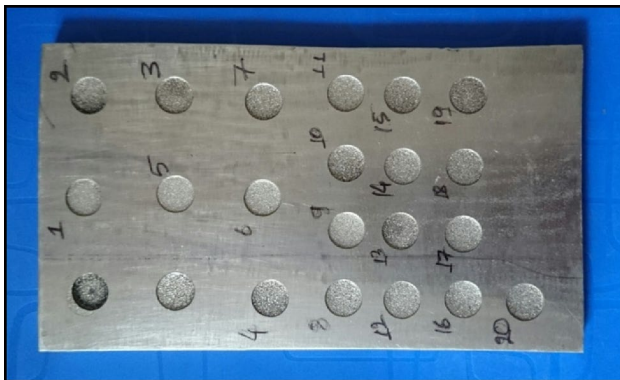
From experimental analysis, it is observed that the MRR increases from 0.160702 gm/min to 0.281006 gm/min with

**Table 4** Process parameters and their levels

Factor	Name	Symbol	Unit	Levels		
A	Peak current	$I_p$	A	9	12	15
B	Pulse-on time	$T_{on}$	$\mu s$	90	120	150
C	Pulse-off time	$T_{off}$	$\mu s$	4	5	6

**Table 5** Experimental data as per design layout

Sl. no	Peak current (A)	Pulse-on time ( $\mu$ s)	Pulse-off time ( $\mu$ s)	MRR (gm/min)	Surface roughness (micron)
1	9.00	90	4.00	0.0943	4.27
2	15.00	90	4.00	0.155	6.65
3	9.00	150	4.00	0.3144	7.18
4	15.00	150	4.00	0.7377	9.82
5	9.00	90	6.00	0.0707	6.85
6	15.00	90	6.00	0.0211	8.95
7	9.00	150	6.00	0.2649	7.43
8	15.00	150	6.00	0.3787	9.23
9	7.00	120	5.00	0.1575	6.44
10	17.50	120	5.00	0.3200	9.98
11	12.00	70	5.00	0.1160	6.53
12	12.00	170	5.00	0.5633	8.33
13	12.00	120	5.00	0.0476	4.22
14	12.00	120	3.32	0.0427	7.44
15	12.00	120	6.68	0.1379	6.81
16	12.00	120	5.00	0.2631	6.44
17	12.00	120	5.00	0.2222	7.34
18	12.00	120	5.00	0.1538	7.35
19	12.00	120	5.00	0.1843	7.23

**Fig. 3** Machined surfaces at different conditions

increase in peak current from 9 to 15 A. The reason was well explained by Shau et al. [15]. Researchers illustrated that when peak current increases, the strength of sparks generates more spark energy or provide higher thermal loading on the both electrodes. Increase in spark energy causes rapid melting and vaporization at the contact of electrode and work-piece resulting in higher MRR. Earlier researchers also suggested that the pulse-on time and peak current are directly related with the discharge energy. Researchers illustrated that at higher pulse-on time the sparking takes place for longer time that have

less sparking frequency resulting in higher rate of melting and evaporation of work-piece, as compare to shorter pulse-on time [23, 24]. Therefore, when pulse-on time increases from 90  $\mu$ s to 150  $\mu$ s, the value of MRR increases from 0.122048 gm/min to 0.430592 gm/min. A decreasing value of MRR from 0.214248 gm/min to 0.13016 gm/min is observed with increase in pulse-off time from 4  $\mu$ s to 6  $\mu$ s. This happened due to decrease in the flushing pressure of the dielectric and decrease in the thermal loading at both electrodes that result in lower value of MRR.

### 3.2 Effect of peak current, pulse-on time and pulse-off time on surface roughness

Visual analysis as well as experimental evaluation has been made to analyse the surface integrity of machined surface that clearly suggests the condition of surface after machining. It is found that the surface roughness increases 6.85  $\mu$ m to 9.01  $\mu$ m as the peak current increases from 9  $\mu$ s to 15  $\mu$ s. An interesting analysis is observed for pulse-on time which interpreted that the value of surface roughness improved with an increase in pulse-on time upto certain limit after that it again start increasing. This happened due to simultaneous action of deposition and removal of material due to crater formation. It is observed that molten materials are deposited on the machined surface and partially

filled up the discharge craters resulting in better surface roughness. But at the higher pulse-on time the formation of craters on the surfaces are larger. These larger craters results in uneven fusion structure, globules of debris, pock-mark and surface crack. Therefore, an increase in surface roughness is observed from 6.93481 μm to 8.37984 μm with increase in pulse-on time from 90 μs to 150 μs. A slight increase i.e. 6.37 μm to 7.81 μm in the value of surface roughness is noticed when pulse-off time increases from 4 μs to 6 μs. This happened due to restrictions that are generated in the flow of debris by the dielectric media. This restriction causes the deposition at the upper layer or at the bottom of electrode. This deposition degraded the surface roughness [25, 26].

### 3.3 ANOVA analysis of material removal rate (MRR)

This study used RSM technique through ANOVA analysis to develop the model of MRR. The ANOVA analysis is shown in Table 6, which shows the value of Model F-value as 12.81 suggest that the model is significant and has a little chance i.e. 0.02% to get larger "Model F-value" due to noise. The analysis also suggest that the model terms are significant because the value of "Prob > F" value is less than 0.0500. The intention of authors is to develop a significant model; therefore non-significant lack of fit is desirable. The analysis also reveals that the Lack of Fit is insignificant because the value of "Lack of Fit F-value" is 2.26. The signal to noise ratio is determine in terms of "Adeq Precision". Hence, signal to noise ratio should be greater than 4. In this study, the ratio is observed as 13.047 that indicates an adequate signal. Hence, the analysis suggests that this

model can be used to navigate the model in the design space. From ANOVA analysis it can be concluded that the pulse-on time and peak current have profound effect on the developed model whereas, a little effect of pulse-off time is observed. The contribution of pulse-on time have observed nearly 60% followed by peak current and square of pulse-on time i.e. 10%. The developed model is shown through Eq. 5. From ANOVA analysis it can be concluded that the interaction plots are made between peak current and pulse-on time, peak current and pulse-off time. The same are shown in below Fig. 4.

$$\begin{aligned}
 \text{MRR} = & -0.95836 - 0.038756 * \text{Peak Current} \\
 & - 0.013768 * \text{Pulse on time} + 0.75804 \\
 & * \text{Pulse off time} + 7.30556E - 004 * \text{Peak Current} \\
 & * \text{Pulse on time} - 0.017492 * \text{Peak Current} \\
 & * \text{Pulse off time} - 1.04583E \\
 & - 003 * \text{Pulse on time} \\
 & * \text{Pulse off time} + 2.44159E \\
 & - 003 * \text{Peak Current}^2 \\
 & + 6.40532E - 005 * \text{Pulse on time}^2 \\
 & - 0.040468 * \text{Pulse on time}^2
 \end{aligned} \tag{5}$$

### 3.4 Interaction plots for MRR

The interaction plot for pulse-on time and pulse-off time is shown in Fig. 4a. From the graph it can be clearly concluded that the effect of pulse-on time is more than pulse-off time on MRR. It can also be concluded from

**Table 6** ANOVA table for MRR

Source	Sum of squares	dof	Mean square	F-value	p-value prob > F	
Model	0.56	9	0.062	12.81	0.0002	Significant
A-peak current	0.049	1	0.049	10.23	0.0095	
B-pulse-on time	0.33	1	0.33	67.26	0.0051	
C-pulse-off time	0.024	1	0.024	5.00	0.0494	
AB	0.035	1	0.035	7.16	0.0233	
AC	0.022	1	0.022	4.56	0.0585	
B <sup>2</sup>	0.048	1	0.048	9.91	0.0104	
C <sup>2</sup>	0.031	1	0.031	6.44	0.0295	
Residual	0.048	10	4.833E-003			
Lack of Fit	0.034	5	6.704E-003	2.26	0.1954	Not significant
Pure Error	0.015	5	2.961E-003			
Cor Total	0.61	19				
R <sup>2</sup>					0.9202	
Adj. R <sup>2</sup>					0.8483	
Pred. R <sup>2</sup>					0.5318	
Adeq. Precision					13.047	

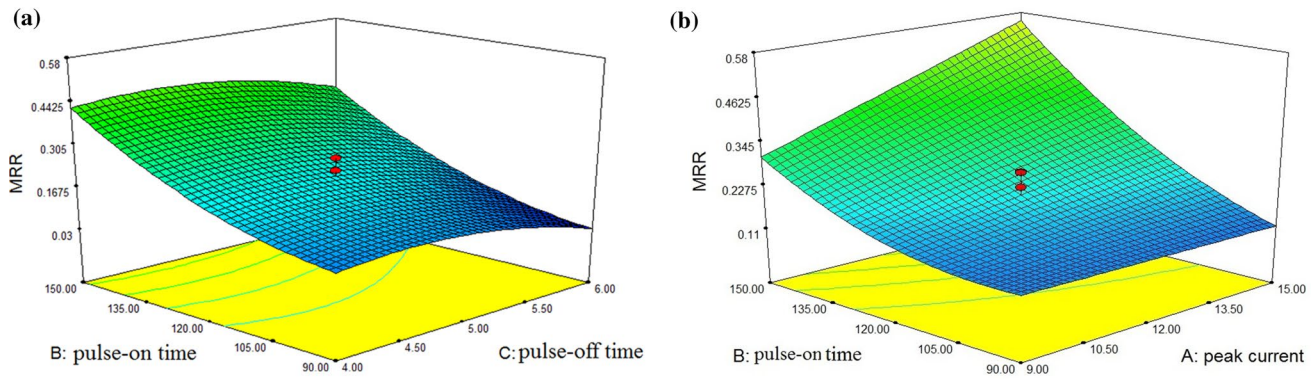


**Fig. 4** a Interaction plot of pulse-on time and pulse-off time on MRR b interaction plot of pulse-on time and peak current on MRR

the graph that higher pulse-on time and lower value of pulse-off time is desirable for getting higher MRR. The interaction plot for pulse-on time and peak current is shown in Fig. 4b. From the graph it can be concluded that both the parameters gives positive effect on MRR i.e. with increase in this parameter the MRR increases. Hence, from the above study it can be concluded that the higher value of pulse-on time and peak current is desirable in order to get higher MRR.

### 3.5 ANOVA analysis of surface roughness

The ANOVA analysis made to develop the model of surface roughness is tabulated in Table 7. The Model F-value observed from the table is 3.16 that suggest the model is significant. The analysis also shows a little chance for larger model F-value due to noise. The values of "Prob > F" is less than 0.0500 indicates that the developed model terms are significant. Lack of Fit is not significant because the value

**Table 7** ANOVA table for surface roughness

Source	Sum of squares	dof	Mean square	F value	p-value prob > F	
Model	39.79	9	4.42	3.16	0.0437	Significant
A-peak current	15.98	1	15.98	11.42	0.0070	
B-Pulse-on time	7.13	1	7.13	5.09	0.0476	
C-Pulse-off time	7.11	1	7.11	5.08	0.0478	
AB	4.500E-004	1	4.500E-004	3.216E-004	0.9860	
AC	0.13	1	0.13	0.093	0.7667	
BC	3.28	1	3.28	2.34	0.1570	
A <sup>2</sup>	1.17	1	1.17	0.84	0.3812	
B <sup>2</sup>	1.348E-003	1	1.348E-003	9.632E-004	0.9759	
C <sup>2</sup>	4.46	1	4.46	3.18	0.1047	
Residual	13.99	10	1.40			
Lack of fit	1.54	5	0.31	0.12	0.9807	Not significant
Pure Error	12.45	5	2.49			
Cor Total	53.78	19				
R <sup>2</sup>					0.7398	
Adj. R <sup>2</sup>					0.5057	
Pred. R <sup>2</sup>					0.4483	
Adeq precision					7.380	

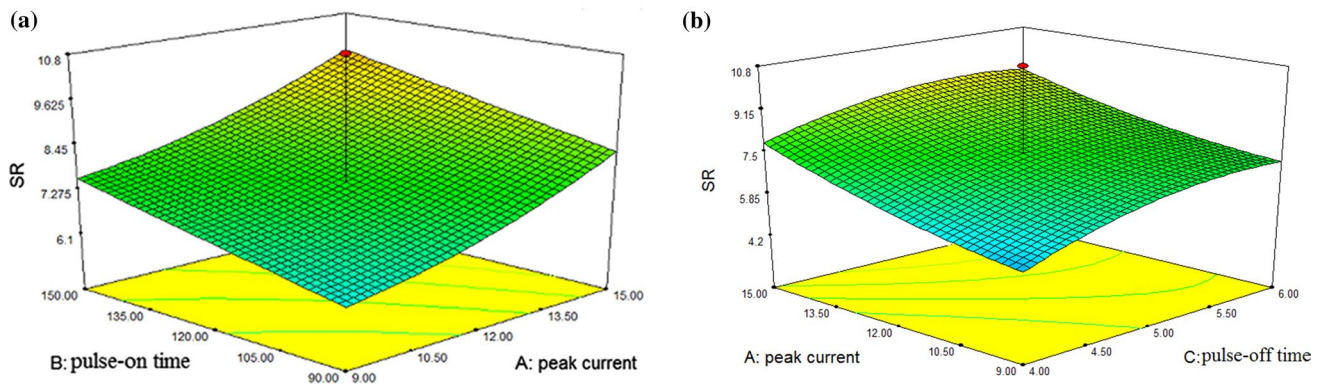


**Fig. 5** **a** Interaction plot of pulse-on time and peak current on surface roughness **b** interaction plot of peak current and pulse-off time on surface roughness

**Table 8** Constraints for optimization of cutting conditions

Condition	Goal	Lower limit	Upper limit
Peak current ( $I_p$ )	Is in range	9	15
Pulse-on time ( $T_{on}$ )	Is in range	90	150
Pulse-off time ( $T_{off}$ )	Is in range	4	6
Surface roughness ( $\mu m$ )	Minimize	4.22	10.8
MRR (gm/min)	Maximize	0.0211	0.7377

of "Lack of Fit F-value" is 0.12 which is desirable. The value of "Adeq Precision" is 7.380 which is greater than 4 indicates a satisfactory signal. The analysis of ANOVA suggests that peak current have profound contribution i.e. 42.12% in the development of model. Pulse-on time and pulse-off time have nearly equal contribution of 18.77% in the developed model. The developed model of surface roughness is shown in Eq. 6. From ANOVA analysis it is found that the interaction effect of peak current and pulse-on time shows highest contribution.

$$\begin{aligned}
 SR = & -27.58622 - 0.19809 * \text{Peak Current} \\
 & + 0.12717 * \text{Pulse on time} \\
 & + 9.35179 * \text{Pulse off time} + 8.3333E \\
 & - 005 * \text{Peak Current} * \text{Pulse on time} \\
 & - 0.042500 * \text{Peak Current} * \text{Pulse off time} \\
 & - 0.21333 * \text{Pulse on time} * \text{Pulse of time} \\
 & + 0.031716 * \text{Peak Current}^2 + 1.0745E \\
 & - 005 * \text{Pulse on time}^2 - 0.55601 \\
 & * \text{pulse off time}^2
 \end{aligned} \tag{6}$$

### 3.6 Interaction plot for surface roughness

The interaction plot for peak current and pulse-on time is shown in Fig. 5a. From the graph it can be clearly

concluded that the effect of peak current is more than pulse-on time on surface roughness. It can also be concluded from the graph that lower peak current and pulse-on time is desirable to get better surface finish. The interaction plot for peak current and pulse-off time is shown in Fig. 5b. The graph shows higher effect of pulse-off time on the surface roughness as compare to peak current. Both parameters shows increasing effect on surface roughness, hence it is desirable to have lower values of said parameters in order to get high surface finish.

Therefore, the above analysis suggests that the higher values of peak current and pulse-on time are desirable in order to get higher MRR whereas, lower values are desirable for high surface finish. Hence, it is dire needed to optimise the processes parameter in order to get high MRR having good surface finish.

### 3.7 Optimization of EDM parameters

The aim of this investigation is to obtain an optimal solution of process parameters in order to get high surface finish and high productivity (i.e. maximum MRR) during the machining process. The constraints used to optimize the input variables are tabulated in Tables 8 and 10 Plan of confirmation experiments and results

Test Machining parameters	Response1	Peak current ( $I_p$ )	Pulse-on time ( $T_{on}$ )	Pulse-off time ( $T_{off}$ )	results	Surface roughness ( $\mu m$ )	Material removal rate (gm/min)
13.491504	Predicted	7.822030	51244	4	Experimental	7.631170	491177
	Error (%)	2.444	159				

Table 9 shows optimal solutions for higher surface integrity and maximum MRR with a desirability of 0.806.

### 3.8 Confirmation experiments

Finally, a set of confirmation runs are performed to verify the prediction ability of the developed models for MRR and surface roughness. Comparisons have been made



**Table 9** Values of parameters for optimization result

Sr. No	Peak current ( $I_p$ )	Pulse-on time ( $T_{on}$ )	Pulse-off time ( $T_{off}$ )	Surface roughness ( $\mu\text{m}$ )	Material removal rate (gm/min)	Remarks
1	13.49	150	4	7.82203	0.512444	Selected

**Table 10** Plan of confirmation experiments and results

Test	Machining parameters			Response		
1	Peak current ( $I_p$ )	Pulse-on time ( $T_{on}$ )	Pulse-off time ( $T_{off}$ )	Results	Surface roughness ( $\mu\text{m}$ )	Material removal rate (gm/min)
	13.49		150	4 Predicted	7.82203	0.512444
				Experimental	7.63117	0.491177
				Error (%)	2.44	4.15

between the values obtained by confirmation run and the predicted values that are obtained from the model are shown in Table 9. The percentage error is found to be less than 5% that indicates the develop model is well suitable for prediction purpose. Therefore, the above analysis clearly suggests that the developed models are suitable for prediction purpose and ready to navigate in space.

## 4 Conclusions

In this investigation a successful attempt has been made to determine the optimal conditions of machining parameters using response surface methodology. The conditions are obtained for minimizing the surface roughness and maximizing the MRR. The pulse-on time shows strongest effect among the other process parameters on MRR, followed by peak current and pulse-off time. The analyses of surface roughness shows that pulse-on time have positive and negative effect on the improvement of surface integrity. It is observed that upto certain values of pulse-on time, there is improvement in surface integrity thereafter, it again start increasing. This happened due to simultaneous action of deposition and removal of material at the time of crater formation. The molten materials are deposited over the machined surface and fills up the discharge craters resulting in the better surface finish. But at the higher pulse-on time the formation of craters on the surfaces are larger. These larger craters results in globules of debris, uneven fusion structure, pockmark and surface crack responsible for degradation in surface integrity. The optimal solution for process parameters are obtained as 13.49 A peak current, 150  $\mu\text{s}$  pulse-on time and 4  $\mu\text{s}$  pulse-off time having MRR as 0.512444 gm/min and SR as 7.82203  $\mu\text{m}$ .

**Acknowledgements** The authors like to thanks director of Sant Longowal Institute of Engineering And Technology to carry out such an innovative work. The authors also like to thanks the director of Goel institute of Technology and Management (GITM) for giving support to publish this work. Finally, the authors thank the staff member of Goel institute of technology and management for giving their consistent support.

## Compliance with ethical standards

**Conflict of interest** On behalf of all authors, the corresponding author states that there is no conflict of interest.

**Open Access** This article is licensed under a Creative Commons Attribution 4.0 International License, which permits use, sharing, adaptation, distribution and reproduction in any medium or format, as long as you give appropriate credit to the original author(s) and the source, provide a link to the Creative Commons licence, and indicate if changes were made. The images or other third party material in this article are included in the article's Creative Commons licence, unless indicated otherwise in a credit line to the material. If material is not included in the article's Creative Commons licence and your intended use is not permitted by statutory regulation or exceeds the permitted use, you will need to obtain permission directly from the copyright holder. To view a copy of this licence, visit <http://creativecommons.org/licenses/by/4.0/>.

## References

1. Guha A, Smyers S, Rajurkar KP, Garimella PS, Konda R (1995) Optimal parameters in electrical discharge machining of copper beryllium alloys. *Proc Int Symp Electromach*, Switz 1:217–224
2. Zeid OA (1997) On the effect of electro-discharge machining parameters on the fatigue life of AISI D6 tool steel. *J Mater Process Technol* 68(1):27–32. [https://doi.org/10.1016/S0924-0136\(96\)02523-X](https://doi.org/10.1016/S0924-0136(96)02523-X)
3. Singh S, Maheshwari S, Pandey PC (2004) Some investigations into the electric discharge machining of hardened tool steel using different electrode materials. *J Mater Process Technol* 149(1):272–277. <https://doi.org/10.1016/j.jmatprotec.2003.11.046>

4. Liao YS, Yu YP (2004) The energy aspect of material property in WEDM and its application. *J Mater Process Technol* 149(1):77–82. <https://doi.org/10.1016/j.jmatprotec.2003.10.031>
5. Salah NB, Ghanem F, Atig KB (2006) Numerical study of thermal aspects of electric discharge machining process. *Int J Mach Tools Manuf* 46(7):908–911. <https://doi.org/10.1016/j.ijmactool.2005.04.022>
6. Kanlayasiri K, Boonmung S (2007) Effects of wire-EDM machining variables on surface roughness of newly developed DC 53 die steel: Design of experiments and regression model. *J Mater Process Technol* 192:459–464. <https://doi.org/10.1016/j.jmatprotec.2007.04.085>
7. Joshi SN, Pande SS (2011) Intelligent process modeling and optimization of die-sinking electric discharge machining. *Appl Soft Comput* 11(2):2743–2755. <https://doi.org/10.1016/j.asoc.2010.11.005>
8. Singh B, Singh P, Tejpal G, Singh G (2012) An experimental study of surface roughness of h11 steel in EDM process using copper tool electrode. *Int J Adv Res Sci Eng Technol* 3(4):130–133
9. Govindan P, Joshi SS (2012) Analysis of micro-cracks on machined surfaces in dry electrical discharge machining. *JMP* 14(3):277–288. <https://doi.org/10.1016/j.jmapro.2012.05.003>
10. Singh S, Yeh MF (2012) Optimization of abrasive powder mixed EDM of aluminum matrix composites with multiple responses using gray relational analysis. *J Mater Eng Perform* 21(4):481–491. <https://doi.org/10.1007/s11665-011-9861-z>
11. Shayan AV, Afza RA, Teimouri R (2013) Parametric study along with selection of optimal solutions in dry wire cut machining of cemented tungsten carbide (WC-Co). *JMP* 15(4):644–658. <https://doi.org/10.1016/j.jmapro.2013.05.001>
12. Sahu J, Mohanty CP, Mahapatra SS (2013) A DEA approach for optimization of multiple responses in electrical discharge machining of AISI D2 steel. *Procedia Eng* 51:585–591. <https://doi.org/10.1016/j.proeng.2013.01.083>
13. Goswami A, Kumar J (2014) Optimization in wire-cut EDM of Nimonic-80A using Taguchi's approach and utility concept. *JESTECH* 17(4):236–246. <https://doi.org/10.1016/j.jestech.2014.07.001>
14. Muthuramalingam T, Mohan B (2015) A review on influence of electrical process parameters in EDM process. *Arch Civ Mech Eng* 15(1):87–94. <https://doi.org/10.1016/j.acme.2014.02.009>
15. Sahu D, Sahu SK, Jadam T, Datta S (2019) Electro-discharge machining performance of Nimonic 80A: an experimental observation. *Arab J Sci Eng* 44:10155–10167. <https://doi.org/10.1007/s13369-019-04112-1>
16. Huu PN, Long BT, Dung LQ, Toan ND, Muthuramalingam T (2019) Multi-criteria decision making using preferential selection index in titanium based die-sinking PMEDM. *J Korean Soc Precis Eng* 36(9):793–802. <https://doi.org/10.7736/KSPE.2019.36.9.793>
17. Huu PN, Van DN, Van BP (2019) Application of response surface methodology for evaluating material removal in rate die-sinking EDM roughing using copper electrode. *Sci Technol Develop J Eng Technol* 1(1):20–27. <https://doi.org/10.15419/stdjet.v1i1.523>
18. Huu PN, Tien LB, Duc QT (2019) Multi-objective optimization of process parameter in EDM using low-frequency vibration of workpiece assigned for SKD61. *Sādhanā* 44:211. <https://doi.org/10.1007/s12046-019-1185-y>
19. Singh BK, Mondal B, Mandal N (2016) Machinability evaluation and desirability function optimization of turning parameters for Cr<sub>2</sub>O<sub>3</sub> doped zirconia toughened alumina (Cr-ZTA) cutting insert in high speed machining of steel machining. *Ceram Int* 42:3338–3350. <https://doi.org/10.1016/j.ceramint.2015.10.128>
20. Singh BK, Roy H, Mondal B, Roy SS, Mandal N (2019) Measurement of chip morphology and multi criterion optimization of turning parameters for machining of AISI 4340 steel using Y-ZTA cutting inserts. *Measurement* 142:181–194. <https://doi.org/10.1016/j.measurement.2019.04.064>
21. Singh BK, Roy H, Mondal B, Roy SS, Mandal N (2018) Development and machinability evaluation of MgO doped Y-ZTA ceramic inserts for high speed machining of steel. *Mach Sci Technol* 22(6):899–913. <https://doi.org/10.1080/10910344.2017.1415937>
22. Singh BK, Ghosh K, Roy SS, Mondal B, Mandal N (2018) Correlation between microstructure and mechanical properties of YSZ/Al<sub>2</sub>O<sub>3</sub> ceramics and its effect on high speed machining of steel. *Trans Indian Ceram Soc* 77(4):219–225. <https://doi.org/10.1080/0371750X.2018.1528889>
23. Goswami A, Kumar J (2014) Optimization in wire-cut EDM of Nimonic-80A using Taguchi's approach and utility concept. *Int J Eng Sci Technol* 17:236–246. <https://doi.org/10.1016/j.jestech.2014.07.001>
24. Thakur A, Gangopadhyay S (2015) State-of-the-art in surface integrity in machining of nickel-based super alloys. *Int J Mach Tools Manuf* 100:25–54. <https://doi.org/10.1016/j.ijmactool.2015.10.001>
25. Choudhury IA, El-Baradie MA (1998) Machinability of nickel-base super alloys: a general review. *J Mater Process Technol* 77:278–284. [https://doi.org/10.1016/S0924-0136\(97\)00429-9](https://doi.org/10.1016/S0924-0136(97)00429-9)
26. Unune DR, Singh H (2017) Parametric modeling and optimization for abrasive mixed surface electro discharge diamond grinding of Inconel 718 using response surface methodology. *Int J Adv Manuf Technol* 93:3859–3872. <https://doi.org/10.1007/s00170-017-0806-z>

**Publisher's Note** Springer Nature remains neutral with regard to jurisdictional claims in published maps and institutional affiliations.